


## Original Article

# Quantification of intrinsic optical signals in the outer human retina using optical coherence tomography

Alina Messner,<sup>1,2</sup> Valentin Aranha dos Santos,<sup>1</sup> Hannes Stegmann,<sup>1,3</sup> Stefan Puchner,<sup>1</sup> Doreen Schmidl,<sup>4</sup> Rainer Leitgeb,<sup>1</sup> Leopold Schmetterer,<sup>1,3,4,5,6,7,8,9</sup> and René M. Werkmeister<sup>1,3</sup> 

<sup>1</sup>Center for Medical Physics and Biomedical Engineering, Medical University of Vienna, Vienna, Austria. <sup>2</sup>Department of Biomedical Imaging and Image-Guided Therapy, Medical University of Vienna, Vienna, Austria. <sup>3</sup>Christian Doppler Laboratory for Ocular and Dermal Effects of Thiomers, Medical University of Vienna, Vienna, Austria. <sup>4</sup>Department of Clinical Pharmacology, Medical University of Vienna, Vienna, Austria. <sup>5</sup>Singapore Eye Research Institute, The Academia, Singapore. <sup>6</sup>SERI-NTU Advanced Ocular Engineering (STANCE) Program, Nanyang Technological University, Singapore. <sup>7</sup>School of Chemical and Biomedical Engineering, Nanyang Technological University, Singapore. <sup>8</sup>Ophthalmology and Visual Sciences Academic Clinical Program, Duke-NUS Medical School, Singapore. <sup>9</sup>Institute of Molecular and Clinical Ophthalmology, Basel, Switzerland

Address for correspondence: René M. Werkmeister, Center for Medical Physics and Biomedical Engineering, Medical University of Vienna, Währinger Gürtel 18–20/4L, 1090 Vienna, Austria. rene.werkmeister@meduniwien.ac.at

**Intrinsic optical signals constitute a noninvasive biomarker promising the objective assessment of retinal photoreceptor function. We employed a commercial optical coherence tomography (OCT) system and an OCT signal model for evaluation of optical path length (OPL) changes in the temporal outer retina of five healthy subjects during light adaptation. Data were acquired at 30 time points, in ambient light and during long duration stimulation with white light, and analyzed, employing a signal model based on the sum of seven Gaussian curves corresponding to all relevant anatomical structures of the outer retina. During light stimulation, mean OPL between rod outer segment tips (ROST) and the retinal pigment epithelium (RPE) decreased by  $21.4 \pm 3.5\%$ . Further, OPL between the external-limiting membrane (ELM) and the RPE decreased by  $5.2 \pm 0.9\%$  versus baseline, while OPL between ELM and ROST showed an initial decrease by  $2.1 \pm 1.6\%$  versus baseline and, thereafter, increased by  $2.8 \pm 2.1\%$  versus baseline. Thus, the presented approach allowed for assess to dynamic changes in the outer retina in response to light. The change in the subretinal space occurring in the context of light adaptation could be measured using a standard OCT platform and a dedicated signal model.**

**Keywords:** intrinsic optical signals; optical coherence tomography; photoreceptors; optophysiology; signal analysis

## Introduction

Optical coherence tomography (OCT) is a contactless imaging technique that has revolutionized ophthalmic diagnosis and has become invaluable for clinical practice. It provides cross-sectional and volumetric image data of the retina and, in addition to these structural parameters, allows for noninvasive assessment of functional parameters *in vivo*, using information about amplitude and phase of back-reflected and back-scattered light.<sup>1</sup>

Optophysiology comprises tools and technologies that, based on optical methods, such as OCT, measure stimulus-evoked changes of optical properties in living tissue.<sup>2–4</sup> In the retina, these stimuli are mainly generated by the illumination with visible light. The evoked changes, called intrinsic optical signals (IOS), can serve as an indicator of the state of the photoreceptor function, making them a promising biomarker for early detection of retinal diseases.<sup>2,5</sup>

doi: 10.1111/nyas.14721

Ann. N.Y. Acad. Sci. 1510 (2022) 145–157 © 2021 The Authors. *Annals of the New York Academy of Sciences* published by Wiley Periodicals LLC on behalf of New York Academy of Sciences

145

This is an open access article under the terms of the Creative Commons Attribution-NonCommercial License, which permits use, distribution and reproduction in any medium, provided the original work is properly cited and is not used for commercial purposes.

Recently, increased interest has led to various studies<sup>6,7</sup> reporting on morphological changes in the outer retina after light stimulation, which present themselves as alterations in the OCT signal amplitude<sup>8,9</sup> or in the optical path length<sup>10</sup> (OPL) between different boundaries in cross-sectional OCT images. Light stimulation protocols and imaging approaches differ between studies and two major findings that are seemingly contradictory have been postulated. While, on the one hand, an increase in the OPL of photoreceptor outer segments (PROS) after light stimulation has been reported in several human<sup>11–14</sup> and animal studies,<sup>15,16</sup> others found an OPL decrease between inner segment/outer segment (IS/OS) junction and retinal pigment epithelium (RPE).<sup>5,17</sup>

The definition of landmarks for measuring retinal changes in response to light stimulation remains challenging, because the detectability of structures is highly variable between scans, platforms, location in the retina, angle of the beam to the retina, and patients. Anatomically, the PROS are limited inwardly by the IS/OS junction and outwardly by the PROS tips.<sup>18</sup> The external-limiting membrane (ELM), a reflective band revealed in OCT and formed by adherent junctions where the Müller cell's apical processes attach to the photoreceptor IS and to each other,<sup>19</sup> is often used as an inner reference for measuring outer retinal structures as well.<sup>20,21</sup> Using the RPE signal as a landmark for the outer PROS limit poses a certain difficulty: The RPE as an adjacent structure is not part of the photoreceptor itself and, therefore, the distance between their boundaries cannot be assumed to remain constant during light stimulation.

An effect of light stimulation on the hydration of the subretinal space, the space between the PROS themselves and between PROS and RPE, has already been reported in animals and in *in vitro* experiments.<sup>16,22–26</sup> In addition, DeLint *et al.* found reflectance changes in the human fovea, but not in the periphery, in response to light stimuli, which they deduced to stem from changes in the refractive index between the disks of the cone OS and the subretinal space.<sup>27</sup> In our previous study in healthy humans, we showed that the OPL between ROST and RPE changes after light stimulation—most likely due to an adjustment in the subretinal space.<sup>17</sup> The study protocol included measurements in the temporal retina of healthy volunteers,

thus targeting mostly rod photoreceptor cells. This differentiation is of particular importance, since, depending on the location on the ocular fundus, rods and cones are present in varying proportions and therefore contribute differently to the PROS signal. This arises from their different morphological and physiological properties: since the cone photoreceptors are shorter than the rods, the ROST are closer to the RPE, while the cone outer segment tips (COST) appear to lie closer to the IS/OS junction.<sup>28</sup> Depending on the incidence angle of the probe beam and the resolution of the imaging system, ROST and COST can be visualized as two distinct reflective layers in the peripheral retina.<sup>12</sup> Measuring light-related changes in the peripheral outer retina is especially interesting in the context of diabetic retinopathy or age-related macular degeneration (AMD). In the former, a dysregulation of the light adaptation-related subretinal space hydration has been shown using OCT in mice,<sup>29</sup> while in the latter, pathological lipid deposition was reported not only to occur between RPE and choroid (Cho), but also in the subretinal space.<sup>30</sup> Rod photoreceptors are the first to be affected in AMD,<sup>31</sup> and it has been proposed that their impaired dark adaptation might be one of the first signs that can be used as a biomarker for disease onset.<sup>30,32</sup> To our knowledge, there are only few studies reporting on the assessment of rod OS changes during light and dark adaptation with OCT in the human retina.<sup>12,13,17</sup>

In the current study, we aimed to refine the analysis for the detection and tracking of position changes of outer retinal layers, particularly ROST and RPE, employing our long duration stimulation protocol in healthy subjects. The evaluation is based on modeling the OCT depth profiles by fitting normal distribution curves and observing their position changes over time. With this approach, we quantitatively evaluate the decrease in OPL of the subretinal space in the context of light stimulation and compare the results to those yielded by our previously reported approach.

## Methods

The analysis of OCT signals was based on a study at the Center of Medical Physics and Biomedical Engineering at the Medical University of Vienna that has previously been reported. The study was approved by the local ethics board of the

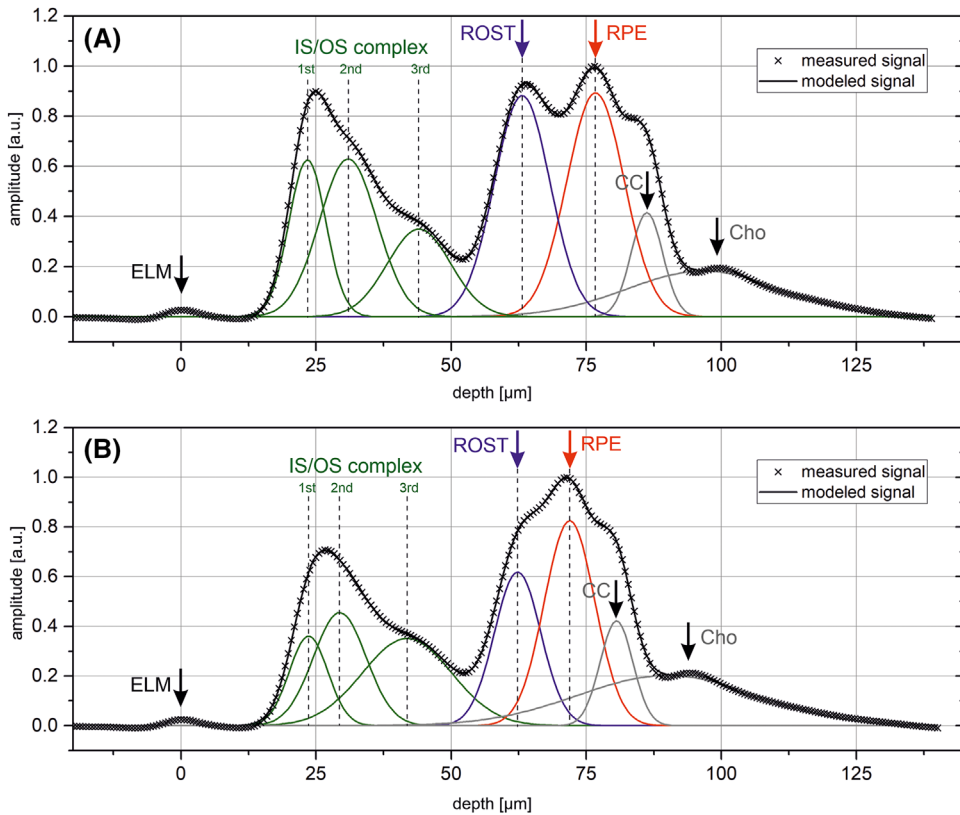


**Figure 1.** Slope corrected A-scan averages with OCT signal modeling by summation of seven Gaussian curves of an individual subject before and after light stimulation. Gray crosses represent the measured data points, and the black line is the summation of the individual model curves (green, blue, red, and gray lines). (A) Measurement during ambient room light before light stimulation. Two peaks that can be attributed to the ROST and RPE can be clearly distinguished. (B) Measurement during white light stimulation. The ROST peak merges with the RPE signal. Its position can be estimated through the model. ELM, external-limiting membrane; IS/OS, inner segment/outer segment complex; ROST, rod outer segment tips; RPE, retinal pigment epithelium; CC, choriocapillaris; Cho, choroid.

Medical University of Vienna and the competent authorities and was performed in adherence to the Declaration of Helsinki<sup>33</sup> and to the Good Clinical Practice guidelines. Study participants gave their written informed consent after explanation of the rationale of the study. Subjects underwent a general medical examination and standard eye examination including perimetry before measurements. To obtain pupil dilation, ensuring that a defined amount of light impinges onto the retina, the study eye received one drop of Mydraticum 0.5% (AGEPHA Pharma s.r.o., Senec, Slovakia). The experimental setup and the measurement protocol have been described in detail previously.<sup>17</sup> Briefly, a commercially available OCT platform (Cirrus HD-OCT 4000, Zeiss Meditec, Jena, Germany)

was employed to acquire OCT image data of the temporal retina of five healthy subjects. The system operates at a central wavelength of 840 nm and provides physical axial and lateral resolutions of approximately 5 and 15  $\mu\text{m}$ , respectively. The pixel resolution of the OCT depth profile after zero padding is 0.567  $\mu\text{m}/\text{pixel}$ . Fifteen baseline measurements, each comprising a volumetric data set with a size of  $320 \times 300 \times 1024$  voxels covering an area of  $3.0 \times 2.4 \text{ mm}^2$  on the temporal retina at an eccentricity of approximately 14 degrees, were performed in ambient room light and with a pause of 1 min between them. On the basis of the work of Thomas and Lamb<sup>34</sup> and considering a pupil diameter of 7 mm and an approximate luminance of 1000  $\text{cd}/\text{m}^2$  at the walls in the laboratory, a fraction

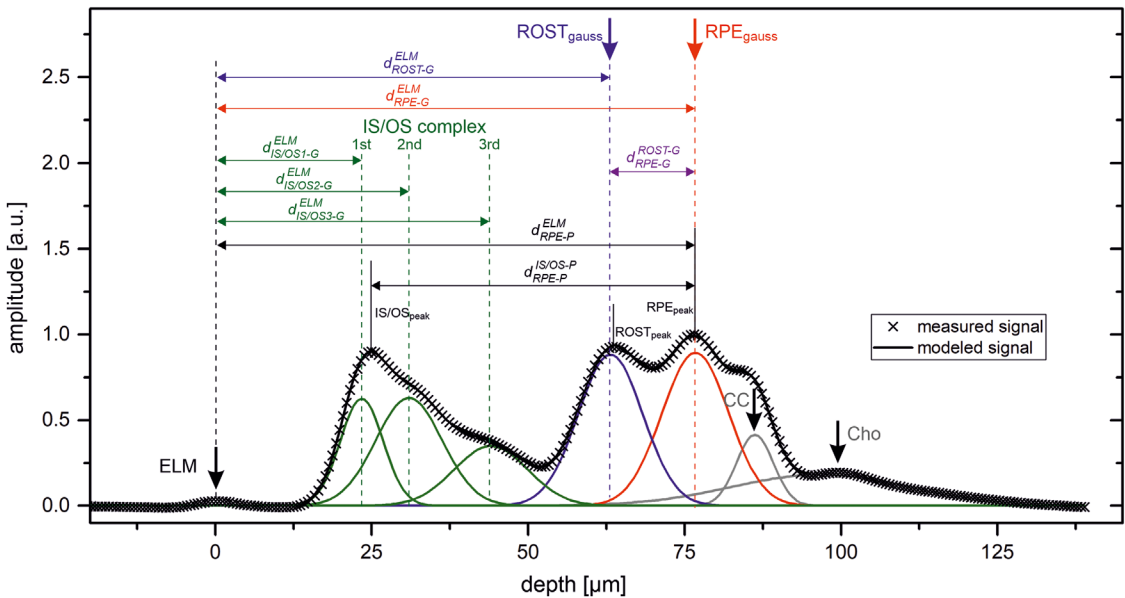


**Figure 2.** Positions of retinal boundaries in the OCT amplitude signal and the OCT signal model and corresponding distances to the ELM as internal reference.

of 62% of rod photo pigment was bleached under ambient light conditions. Then, measurements were repeated after the retina was exposed to a wide field light stimulus of  $35 \times 10^3$  cd/m<sup>2</sup> luminance. Before the first measurement, the stimulus was applied for 5 min, which bleached about 98% of rod photopigment. For the subsequent 14 times, the light stimulus was then applied for 1 min in between OCT measurements, leading to a fractional bleach >99%. The described protocol resulted in 15 measurements during the light stimulation period, where each OCT measurement took approximately 10 seconds. Lateral stabilization of the acquired volumetric data set on the intended region of interest was assured by tracking software implemented in the OCT system and confirmed retrospectively during image analysis by the monitoring of image landmarks like small vessels in the en face projections of the OCT image data set (see Fig. S1, online only).

For the creation of a single, comprehensive retinal depth profile, all A-scans of one measurement were registered to the position of the maximum of the IS/OS junction and averaged (referred to as *A-scan average* from this point), as has been described previously.<sup>17,35,36</sup> In Figure 1, example A-scan averages, represented by the crosses, of one measure-

ment before (Fig. 1A) and one after (Fig. 1B) light stimulation are depicted. As can be seen, before light stimulation, two peaks in the ROST/RPE signal-complex are revealed, representing most likely the ROST and RPE, respectively. However, in the A-scan average during the light stimulation phase, the corresponding reflective bands merge and only one peak is detectable. In our initial approach for analysis of the data, the OPL between the highest peak of the IS/OS junction complex and the ROST/RPE signal complex at baseline condition and during light stimulation were determined. In the current manuscript, we expand the signal analysis to investigate the contribution of the different retinal layers and the light-induced OPL change in between them. In order to determine the position of the ROST peak hidden in the ROST/RPE signal complex, a signal model for the A-scan averages, based on the sum of seven Gaussian curves and linear slope correction for compensation of the sensitivity decay of the OCT signal, was developed in the software Origin (OriginPro, Version 2019b. OriginLab Cooperation, Northampton, MA), using the “multiple peak fitting” function and employing the Levenberg–Marquardt algorithm for determination and optimization of the Gaussian curve parameters.

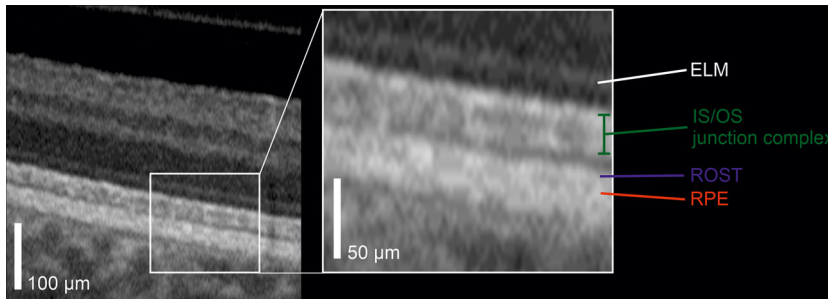


**Figure 3.** Example cross-sectional image of the peripheral temporal retina provided by the OCT platform used in this study. ELM, external-limiting membrane; IS/OS junction complex, inner segment/outer segment junction complex; ROST, rod outer segment tips; RPE, retinal pigment epithelium.

In this OCT signal model, the IS/OS junction and the ROST/RPE signal complex are represented by three (IS/OS1, IS/OS2, and IS/OS3) and two curves respectively, while the signal arising from the choriocapillaris (CC) and the Cho can be modeled by one curve each. Contrary to our initial approach, using the maximum of the IS/OS junction complex as reference, the new model employs the ELM as robust inner reference for comparison of other peak positions before and after light stimulation. In Figure 2, the position of the different boundaries in the outer retina both in the OCT intensity signal and in the introduced signal model and their respective distances to each other are depicted.

To investigate alterations in the modeled averaged A-scan related to the measurement position at the ocular fundus, in two subjects, additional volumetric OCT data at five locations with distances of 0, 3.5, 7, 10.5, and 14 degrees from the macula were acquired. These measurements were only performed in ambient room light.

OPLs in the Results section are given as  $d_B^A$ , where  $A$  and  $B$  indicate the corresponding layers and  $d$  the distance between them. Relative OPL changes are given as  $\Delta d_B^A$ , with  $A$  and  $B$ , again, indicating the outer retinal layers and  $\Delta d$  the change of the distance with respect to the average of all baseline measurements ( $t = -14 \dots 0$ ), in the following referred to as “baseline.”

### Statistical analysis

Statistical tests were performed in SPSS (IBM SPSS Statistic 26.0). The mean OPL before and during the light stimulation period were compared using a paired  $t$ -test and the Bonferroni method was used to adjust for multiple testing. The intraclass cor-

relation coefficient (ICC) was calculated using all measurements in a two-way, mixed alpha model of absolute agreement. A  $P$ -value of 0.05 was considered the level of significance. For the average time courses of all subjects, due to the small sample size, only a qualitative and quantitative analysis without testing for statistical significance is presented.

### Results

The measurement data of five healthy subjects (three women and two men) with a mean age of  $28 \pm 2$  years were included in the analysis. In Figure 3, an example cross-sectional OCT image of the peripheral retina, depicting the outer retinal layers assessed in the current study, is shown.

In order to test the precision of the peak detection using the signal model based on Gaussian curves, position values of the highest peak in the A-scan average, which represents the RPE (initial approach from previous report),<sup>17</sup> were compared with the corresponding position of that layer in the signal model. For all subjects, the mean positions of the RPE peak position ( $RPE_{peak}$ ) and the RPE position in the signal models ( $RPE_{gauss}$ ) of 30 measurements deviated by a mean of  $0.22 \pm 1.10 \mu\text{m}$ . The ICC for single measures was 0.977 and for average measures 0.988 (both  $P < 0.001$ ), showing excellent agreement of the RPE position in both approaches.

### ROST to RPE

On the basis of the signal model, peaks representing the ROST and RPE could be assessed at each time point before (baseline,  $t = -14 \dots 0$ ) and during the light stimulation period ( $t = 1 \dots 15$ ). Example A-scan averages of both a baseline measurement and a measurement during the stimulation period



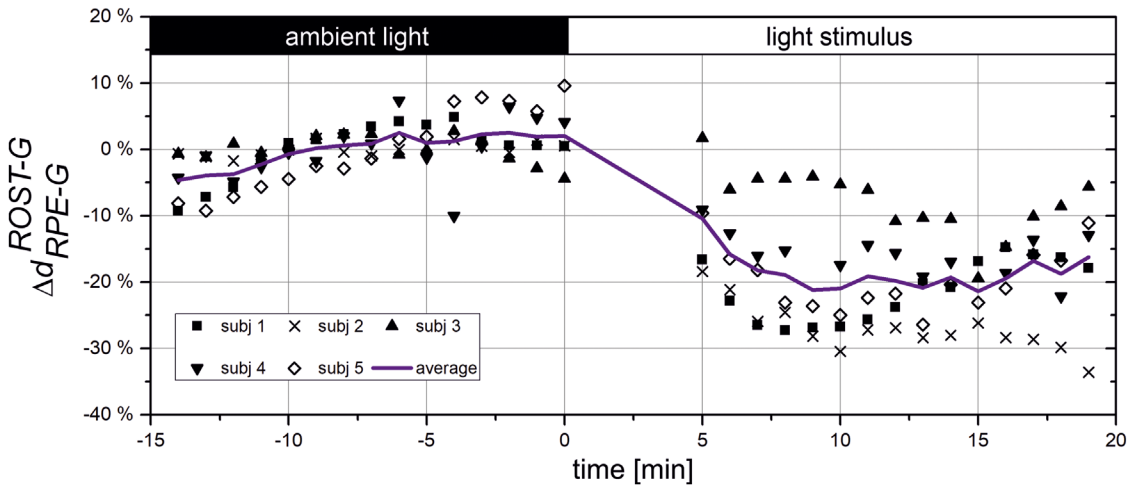


**Figure 4.** Relative distance change between the peaks attributed to ROST and RPE. The purple curve represents the average of all subjects, while the values of single subjects and measurements are given as symbols. Each subject curve is offset so that the mean value of the baseline ( $t = -14$  min...0 min) corresponds to 0%. The time axis represents the measurement time relative to the stimulation onset. The stimulation period started directly after the last measurement in ambient room light. Linear interpolation was performed between measurement time points.

are depicted in Figure 1. The OPL between the two peaks decreased distinctly in all five subjects during the light stimulation period (Fig. 4). At baseline, the average  $d_{ROST-G}^{RPE-G}$  for all subjects was  $11.6 \pm 0.2 \mu\text{m}$ , while the distance reached a minimum of  $9.3 \pm 1.2 \mu\text{m}$  after a cumulative stimulation time of 15 min, which corresponds to a maximum relative decrease of  $21.4 \pm 3.5\%$ . The mean value of the absolute individual subjects' minima was  $8.5 \pm 0.7 \mu\text{m}$ , corresponding to a decrease of  $26 \pm 5\%$ .

The mean standard deviation of the baseline was 3%. The highest deviations between individual subjects' measurements were found directly after the first 5 min-light stimulation, leading to a standard deviation of 12.5% at this time point.

#### ELM to RPE

The average OPL  $d_{RPE-G}^{ELM}$  over all subjects at baseline in ambient light was  $75.2 \pm 2.2 \mu\text{m}$ . After a cumulative light stimulation time of 9 min, this distance decreased by  $5.2 \pm 0.9\%$  to a value of  $71.3 \pm 1.9 \mu\text{m}$  (Fig. 5E). The relative intrasubject standard deviation of the baseline averaged over all subjects was 0.5%. The average value  $\Delta d_{RPE-G}^{ELM}$  of individual subjects' maximum change was  $4.0 \pm 0.6 \mu\text{m}$ , corresponding to a relative OPL decrease of  $5.3 \pm 0.8\%$ . To compare these numbers with our previously published approach based on the IS/OS as reference,<sup>17</sup>

the relative changes were recalculated using the OPL of the IS/OS complex maximum (instead of the ELM position) to the RPE peak position, that is,  $d_{RPE-G}^{IS/OS-P}$ . In the manuscript at hand, after 9 min of cumulative light stimulation, the average  $d_{RPE-G}^{IS/OS-P}$  decreased by  $5.9 \pm 1.3 \mu\text{m}$ , which corresponds to a relative change of  $12.0 \pm 2.4\%$  and thus is in good agreement with our previous data. The average maximum change occurring at slightly different time points in individual subjects was  $6.0 \pm 1.1 \mu\text{m}$  ( $12.2 \pm 2.1\%$ ). The relative intrasubject standard deviation of the baseline averaged over all subjects was 0.8%. Using our signal model, we found that the three peaks constituting the IS/OS junction undergo individual position changes after light stimulation (Fig. 5A–C). Beyond 9 min of cumulative light stimulation, the  $d_{RPE-G}^{ELM}$  revealed a slow increase approaching the baseline value again. A similar time course was observed for the signals of CC and the Cho (Fig. 5F and G). Intrasubject comparisons of the two different methods for estimation of the boundary positions in the OCT signal of the outer retina during light stimulation are given in Table 1.

#### ELM to ROST

On the basis of the signal model with Gaussian curves, the average baseline OPL  $d_{ROST-G}^{ELM}$  over all subjects was measured to be  $63.6 \pm 1.6 \mu\text{m}$ . After

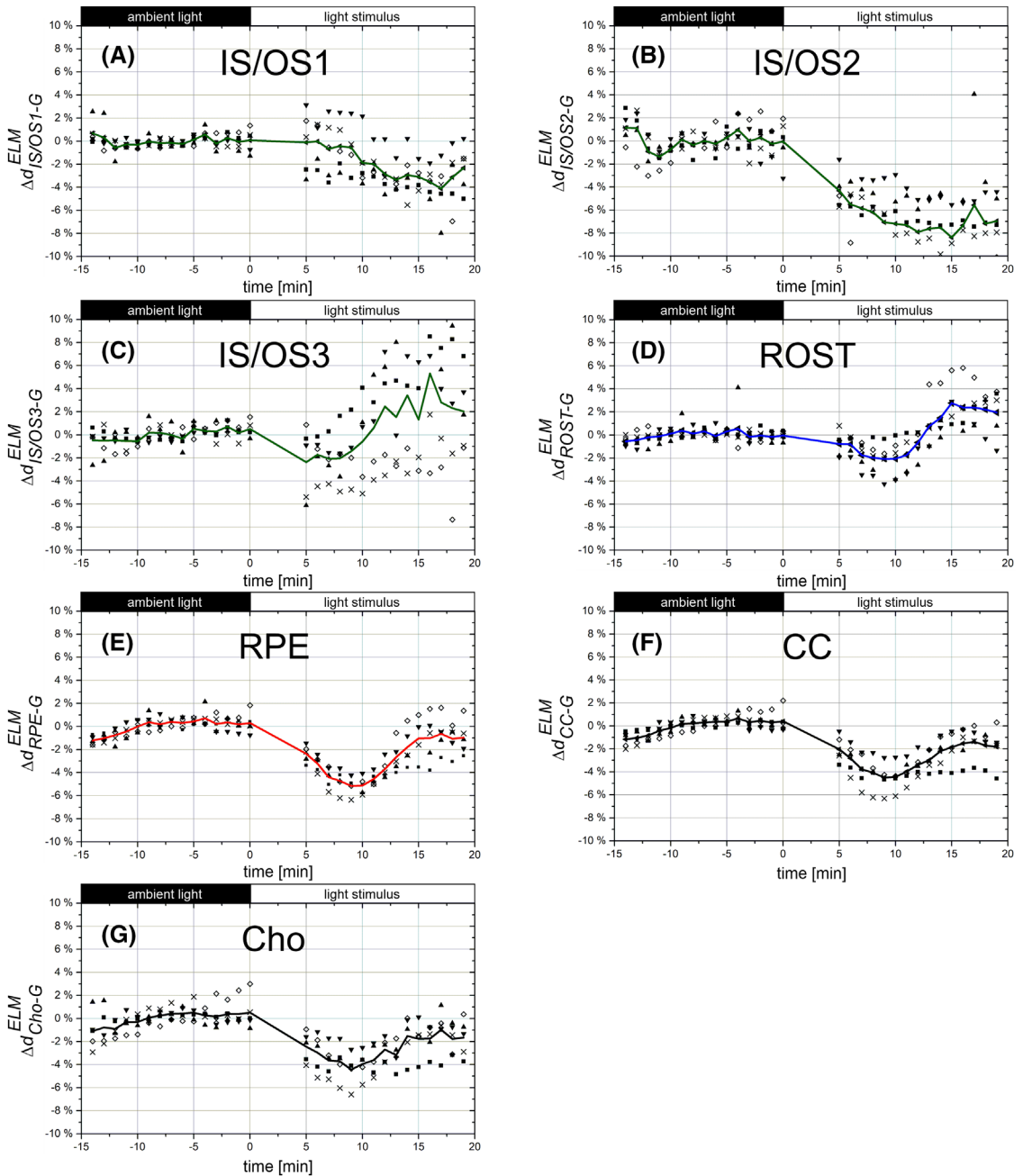


**Figure 5.** OPL changes  $\Delta d_B^{\text{ELM}}$  relative to the baseline value for the fitted Gaussian peaks attributed to IS/OS junction complex (three peaks), ROST, RPE, CC, and choroid. The average of all subjects is given as a line, while the values of single subjects are given as symbols. (A–C) Rather inhomogeneous changes in  $\Delta d_{\text{IS/OS-G}}^{\text{ELM}}$  of the peaks of the IS/OS junction modeling could be observed after light stimulation. The mean of the distance-to-ELM change of the second peak of the IS/OS junction (B) showed the biggest relative change compared with baseline. The time axis represents the measurement time relative to the stimulation onset. The stimulation period started directly after the last measurement in ambient room light. Linear interpolation was performed between measurement time points.

**Table 1.** Comparison of the OPL changes between different retinal boundaries after light exposure as determined by the two different methods for position detection

Subj.		Max. abs. OPL change versus baseline ( $\mu\text{m}$ )	Time to max. OPL change (min)	Mean abs. OPL change versus baseline ( $\mu\text{m}$ )
1	$\Delta d_{RPE-G}^{ELM}$	4.2	9	2.2**
	$\Delta d_{RPE-P}^{ELM}$	4.5	8	2.4**
	$\Delta d_{RPE-P}^{IS/OS-P}$	6.0	8	4.7**
2	$\Delta d_{RPE-G}^{ELM}$	3.5	10	2.6**
	$\Delta d_{RPE-P}^{ELM}$	2.7	7	2.2**
	$\Delta d_{RPE-P}^{IS/OS-P}$	3.6	9	3.0**
3	$\Delta d_{RPE-G}^{ELM}$	2.7	9	1.4*
	$\Delta d_{RPE-P}^{ELM}$	2.3	8	1.0**
	$\Delta d_{RPE-P}^{IS/OS-P}$	4.0	9	2.8**
4	$\Delta d_{RPE-G}^{ELM}$	3.9	10	2.2**
	$\Delta d_{RPE-P}^{ELM}$	3.3	10	2.0*
	$\Delta d_{RPE-P}^{IS/OS-P}$	5.1	10	3.7**
5	$\Delta d_{RPE-G}^{ELM}$	3.4	9	1.1*
	$\Delta d_{RPE-P}^{ELM}$	2.9	10	1.0*
	$\Delta d_{RPE-P}^{IS/OS-P}$	6.6	10	4.7**

\* $P < 0.05$ . \*\* $P < 0.001$ .

NOTE: For easier comparison, the values of the peak-position-approach ("RPE-P") are given for both inner references, the ELM and the maximum of the IS/OS junction complex. The maximum absolute OPL change is the difference between the mean of the baseline measurements and the measurement in the light stimulation period with the largest difference from this mean. The mean absolute OPL change indicates the difference between the mean of the baseline measurements and the mean of the light stimulation period measurements. The  $P$  values correspond to a paired  $t$ -test and are Bonferroni-corrected to adjust for multiple testing.

a cumulative light exposure of 9 min, an average decrease  $\Delta d_{ROST-G}^{ELM}$  by  $2.1 \pm 1.6\%$  to a mean OPL of  $62.3 \pm 2.1 \mu\text{m}$  was observed (Fig. 5D). The mean of the individual subjects' maximum decrease  $1.6 \pm 0.8 \mu\text{m}$  or  $2.6 \pm 1.4\%$ . Thereafter, the average  $d_{ROST-G}^{ELM}$  increased above baseline to a mean value of  $64.7 \pm 1.0 \mu\text{m}$ , which corresponded to an average increase in  $\Delta d_{ROST-G}^{ELM}$  of  $2.8 \pm 2.1\%$ . This was reached after a cumulative light stimulation time of 15 minutes. Here, the mean of the individual subjects' maximum change versus baseline was  $3.7 \pm 1.2\%$  or  $2.3 \pm 0.7 \mu\text{m}$ . The mean standard deviation of the baseline was  $0.6\%$ .

The relative changes before and during the light stimulation period of all peaks of the Gaussian model referenced to the ELM are shown in Figure 5. Qualitative comparison of the time courses reveals similar trends for the position changes of IS/OS1-G and IS/OS2-G and for IS/OS3-G and RPE-G, respectively. While the first two layers show a decreasing OPL with respect to the ELM during light stimulation, the latter pair, during the same time period, exhibits an increase in OPL referred to the ELM. In order to investigate the origin of the opposed OPL changes in the three Gaussian peaks of the IS/OS junction complex, in two subjects, volumetric OCT data were acquired at retinal eccentricities of 0, 3.5, 7, 10.5, and 14 degrees. The averaged A-scans from the different locations of the ocular fundus are shown in Figure 6 and, in both subjects, demonstrate the position-related alteration of the signal of the IS/OS junction complex. For the sake of clarity, only the Gaussian curves of IS/OS3-G are shown and reveal an increase in  $d_{IS/OS3-G}^{ELM}$  with decreasing retinal eccentricity, the magnitude of which exceeds that of the OPL changes in the other modeled boundaries in the OCT signal. All OPL as assessed from the averaged A-scans are given in Table S1 (online only).

## Discussion

The present signal model for the A-scan average, that is, the average OCT depth profile of a region of interest in the peripheral temporal retina, allowed for tracking the position of the peaks attributed to the boundaries of the outer retinal layers during baseline conditions and stimulation of the retina with white light, extracting quantitative parameters of IOS. Particularly the position of the ROST signal, which could not be identified during all time points of the stimulation period in our previous approach on the basis of the detection of the signal peak, could now be determined throughout the measurements. A similar approach employing signal deconvolution was recently reported by Zhang and coworkers for the *in vivo* measurement of the diurnal variation in rod OS length in mice.<sup>37</sup>

The findings obtained by employing the new approach are in good agreement with the previous analysis of the data. A decrease in the OPL between RPE and ROST could be observed in all subjects, confirming our prior interpretation of the data and indicating a mechanism involving a



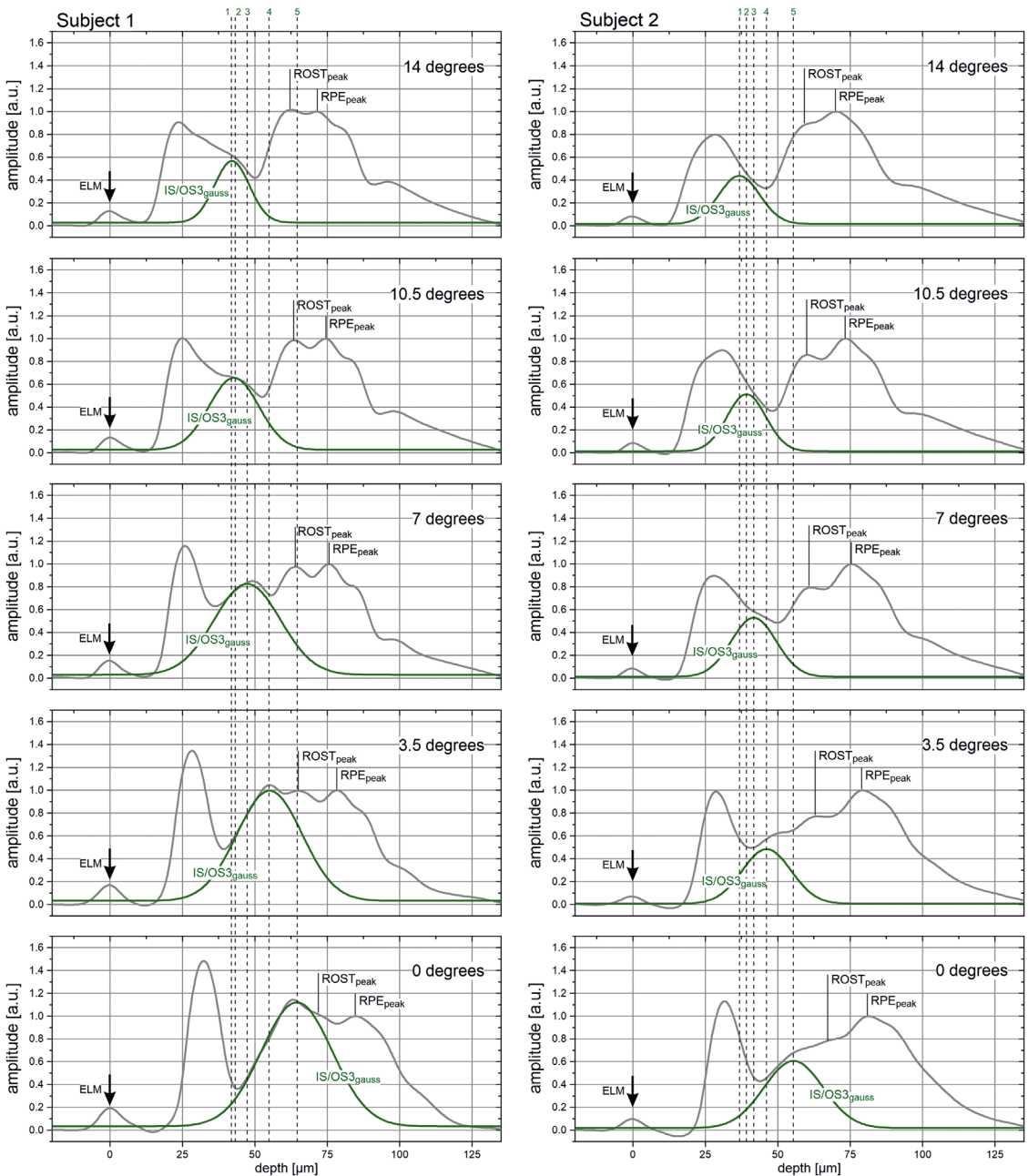


**Figure 6.** Position of the IS/OS3 peak at different retinal eccentricities. The averaged A-scans in the upper panel (14 degrees) correspond to the measurement location employed for the assessment of intrinsic optical signals during white-light stimulation of the retina, while in the lowest panel (0 degrees), the volumetric OCT scan was centered at the macular region.

volumetric change in the subretinal space. In the OCT depth profile, the IS/OS junction represents the inner border of the PROS.<sup>18</sup> Therefore, assessing the OPL between the IS/OS junction complex and the ROST would provide a direct measurement of

the OS length, allowing both straightforward interpretation of light-induced changes in the OS and comparability with other studies. However, in our previous report,<sup>17</sup> employing the signal peaks for measurement of OPL changes in the outer retina,

such a measurement was only possible in the eye adapted to ambient light, whereas during light stimulation, a peak related to the ROST could often not be identified. Since the new signal model allows to determine the position of ROST also during the whole stimulation period, illumination of the retina with white light revealed changes both in the amplitude and, more importantly, also in the depth location of the peaks constituting the IS/OS junction complex. Therefore, the referencing of signals corresponding to other morphological structures to one of these IS/OS junction peaks was deemed unreliable. Instead, the ELM was used as an internal reference for the length changes of the outer photoreceptor segments. Consequently, since the assessed OPL encompasses also the photoreceptor IS, in the report in hand, the position changes of the ROST can only indirectly be interpreted as OPL changes of the OS.

After an initial decline, an increase in OPL between ELM and ROST was observed. In comparison to studies observing OS OPL increases with high time-resolution and using short stimulation times,<sup>11,13</sup> in our experiments, the timeframe leading to the observed increase in OPL is much longer, leading to maximum deflections at the 5 and 15 min mark. Studies employing similar measurement protocols with lower time resolution, but longer duration, found comparable time courses.<sup>5,12</sup> However, comparison of the quantitative extent of the observed OPL change with the findings of previous studies has to be performed with caution. This is due to the aforementioned fact that in the different reports, different outer retinal boundaries and the OPL changes in between them were employed to characterize changes in the photoreceptor OS during light stimulation.

When, hypothetically, instead of the ELM, the second peak of the IS/OS signal complex is used as the internal reference, a light stimulation-induced OPL change between this peak and the ROST position would indicate an elongation of the PROS. By contrast, when employing the third IS/OS peak as the reference, the OPL of the PROS would change much less. Furthermore, measurements were performed in a peripheral area of the retina with a high number of rods. This contrasts with most of the previous studies that focused mainly on the macula region predominantly comprising cone photoreceptors. Therefore, and due to differences in the employed measurement protocols, it is unclear

if the increase observed in the present study and the increase in OS OPL of other studies are mediated by the same mechanism.

An interesting finding is the parallel position shift of several of the observed boundaries (Fig. 5). As expected, the first and second Gaussian peaks composing the IS/OS junction complex shift almost in parallel; however, the OPL between them seems to decrease. The third peak's course is similar to that of the ROST. In order to investigate the origin of the peaks constituting the IS/OS junction complex, volumetric OCT data were acquired at different retinal eccentricities between the peripheral retina, that is, the region employed for the assessment of IOS in the current study, and the macular region. Analysis of the averaged A-scans revealed an increase of the OPL between ELM and IS/OS3 with decreasing eccentricity. The magnitude of this increase was larger than that of the change of the other modeled boundaries. In the averaged signal profiles, the IS/OS3 signal migrated in the direction of ROST and RPE the closer the measurement area was to the macula. The most likely explanation could be that this IS/OS3 peak is not part of the rods IS/OS junction, but represents the COST. Several investigators have reported that cone OS length is greatest in the fovea and decreases with increasing retinal eccentricities,<sup>18,38,39</sup> which is consistent with our results where the OPL  $d_{IS/OS3-G}^{IS/OS1-G}$  is largest in the macula, and decreases to the periphery (see Table S1, online only). Since the OS appears to have a constant volume independent of the location at the ocular fundus, the elongation of the foveal cones has been suggested to be linked to the increased packing of the photoreceptors in this region.<sup>39,40</sup> Another finding that supports the hypothesis that the third peak of the IS/OS junction complex corresponds to the COST concerns the signal strength of the individual peaks. The relatively small amplitude of the average peak in our peripheral region of interest for IOS measurement can be indicative for an only low number of cones, while, at smaller eccentricities, an increase of this amplitude, caused by the increase in cone density, can be observed. These observations also help to explain the changes in the IS/OS junction complex during light stimulation, since the cone photoreceptors and its outer segment tips, which are constituting part of the signal complex, are strongly affected by the impinging white light and induce an OPL change of their signal

with respect to the ELM. This also speaks in favor of employing the ELM as an external reference, whose signal itself is not affected by the stimulus.

Movement of rod OS due to light stimulus, as in transient retinal phototropism, has been postulated in other studies<sup>41</sup> and is another interesting observation to be taken into account when interpreting the light-induced changes in the signal complexes. A change of angle of the rod OS with respect to the RPE, such as bending or erecting, would also correspond to a decrease or increase in distance of the ROST layer to the IS/OS or ELM layer and the volume of the subretinal space.

The present study has some limitations that are worth mentioning. Because of the small sample size of five subjects, no statistical test for assessment of the statistical significance of the measured OPL changes was performed. Since we aimed to employ new measurement and data analysis protocols for the assessment of a potential new biomarker, the influence of the intervention on this parameter was not known *a priori*. Therefore, the current experiments were designed as a pilot study in an effort to evaluate both the stimulation protocol and different postprocessing steps for assessment of light-induced changes in retinal morphology. The new approach enabled the evaluation of particular changes in the different OCT signal complexes in the outer retina that were not revealed by the previous approach, which used only the signal maximum of the corresponding signal complex. On the basis of the obtained data and its characteristics, future studies investigating IOS in healthy subjects, for example, investigating local or diurnal variations, or patients suffering from retinal diseases impairing the photoreceptor function, can be planned.

In conclusion, the presented model of the OCT signal of the outer retina provided additional information about the measured IOS in averaged OCT A-scans and could further characterize the reaction to long light stimuli of the peripheral retina. The simplified assessment method that combines a dedicated imaging protocol and signal model for data obtained with a commercially available OCT platform could be easily implemented in clinical routine examinations. The quantitative assessment of changes in subretinal space makes the approach ideally suited for both follow-up measurements in individual subjects and intersubject comparison. Application in a larger group of subjects should be

performed to investigate the precision and reproducibility of the technique. Alternative protocols as well as measurement locations in the retina could be used to further elucidate the affiliation of the boundaries to certain cells or cell parts and related light adaptation processes within the retina. Here, the measured IOS could ultimately serve as biomarkers for the investigation of the health of the outer retina.

## Acknowledgments

A.M., V.A.d.S., D.S., R.L., L.S., and R.M.W. contributed to conception and design of the work. A.M., H.S., S.P., and R.M.W. acquired the data. A.M., V.A., H.S., and R.M.W. conducted the analyses and interpreted the results. A.M. and R.M.W. wrote the initial draft. All authors participated in revising the manuscript and approved the submitted version. R.M.W. accepts responsibility for the integrity of the data analyzed. The research has been funded by the Vienna Science and Technology Fund (WWTF) through project LS14-067. We thank Dr. Martin Kallab and Dr. Nikolaus Hommer for their help with the screening visits, Alexandra Rauch and Dr. Gerhard Garhöfer for their help with organizational matters, and Dr. Alexandre Tumlinson from Carl Zeiss Meditec Inc. for helping with the raw data access to the software.

## Supporting information

Additional supporting information may be found in the online version of this article.

**Figure S1.** Optical coherence tomography en face projections of the measurement series for evaluation of intrinsic optical signals in the outer retina (A) under baseline condition and (B) during stimulation with white light. Landmarks like small retinal vessels and their bifurcation are visualized particularly in the upper part of the images. On the basis of the image features, the lateral stabilization of the OCT data acquisition in the retinal region of interest was confirmed. Scale bars represent 1 mm.

**Table S1.** Optical path length (OPL) in the outer retina at different retinal eccentricities. Path lengths are assessed on the basis of the signal model employing seven Gaussian curves for representation of the different boundaries revealed in the averaged A-scan. Rows “−14deg” show the path length changes in comparison to a retinal eccentricity of 14 degrees,

representing the region where light stimulation experiments were performed. OPL are given in  $\mu\text{m}$ .

## Competing interests

The authors declare no competing interests.

## References

- Drexler, W. & J.G. Fujimoto. 2008. *Optical Coherence Tomography*. Berlin Heidelberg: Springer.
- Yao, X. & B. Wang. 2015. Intrinsic optical signal imaging of retinal physiology: a review. *J. Biomed. Opt.* **20**: 090901.
- Smedemark-Margulies, N. & J.G. Trapani. 2013. Tools, methods, and applications for optophysiology in neuroscience. *Front. Mol. Neurosci.* **6**: 18.
- Bizheva, K., R. Pflug, B. Hermann, *et al.* 2006. Optophysiology: depth-resolved probing of retinal physiology with functional ultrahigh-resolution optical coherence tomography. *Proc. Natl. Acad. Sci. USA* **103**: 5066–5071.
- Abramoff, M.D., R.F. Mullins, K. Lee, *et al.* 2013. Human photoreceptor outer segments shorten during light adaptation. *Invest. Ophthalmol. Vis. Sci.* **54**: 3721–3728.
- Yao, X. & T.H. Kim. 2020. Fast intrinsic optical signal correlates with activation phase of phototransduction in retinal photoreceptors. *Exp. Biol. Med.* **245**: 1087–1095.
- Pandiyani, V.P., X. Jiang, A. Maloney-Bertelli, *et al.* 2020. High-speed adaptive optics line-scan OCT for cellular-resolution optoretinography. *Biomed. Opt. Express* **11**: 5274–5296.
- Ma, G., T. Son, T.H. Kim & X. Yao. 2021. *In vivo* optoretinography of phototransduction activation and energy metabolism in retinal photoreceptors. *J. Biophotonics* **14**: e202000462.
- Son, T., T.H. Kim, G. Ma, *et al.* 2021. Functional intrinsic optical signal imaging for objective optoretinography of human photoreceptors. *Exp. Biol. Med.* **246**: 639–643.
- Ma, G., T. Son, T.H. Kim & X. Yao. 2021. Functional optoretinography: concurrent OCT monitoring of intrinsic signal amplitude and phase dynamics in human photoreceptors. *Biomed. Opt. Express* **12**: 2661–2669.
- Hillmann, D., H. Spahr, C. Pfaffle, *et al.* 2016. *In vivo* optical imaging of physiological responses to photostimulation in human photoreceptors. *Proc. Natl. Acad. Sci. USA* **113**: 13138–13143.
- Lu, C.D., B. Lee, J. Schottenhamml, *et al.* 2017. Photoreceptor layer thickness changes during dark adaptation observed with ultrahigh-resolution optical coherence tomography. *Invest. Ophthalmol. Vis. Sci.* **58**: 4632–4643.
- Azimipour, M., D. Valente, K.V. Vienola, *et al.* 2020. Investigating the functional responses of human cones and rods with a combined adaptive optics SLO-OCT system. In SPIE BiOS, San Francisco, CA.
- Azimipour, M., D. Valente, K.V. Vienola, *et al.* 2020. Optoretinogram: optical measurement of human cone and rod photoreceptor responses to light. *Opt. Lett.* **45**: 4658–4661.
- Zhang, P., R.J. Zawadzki, M. Goswami, *et al.* 2017. *In vivo* optophysiology reveals that G-protein activation triggers osmotic swelling and increased light scattering of rod photoreceptors. *Proc. Natl. Acad. Sci. USA* **114**: E2937–E2946.
- Li, Y., R.N. Fariss, J.W. Qian, *et al.* 2016. Light-induced thickening of photoreceptor outer segment layer detected by ultra-high resolution OCT imaging. *Invest. Ophthalmol. Vis. Sci.* **57**: OCT105–111.
- Messner, A., R.M. Werkmeister, G. Seidel, *et al.* 2019. Light-induced changes of the subretinal space of the temporal retina observed via optical coherence tomography. *Sci. Rep.* **9**: 13632.
- Jonnal, R.S., O.P. Kocaoglu, R.J. Zawadzki, *et al.* 2014. The cellular origins of the outer retinal bands in optical coherence tomography images. *Invest. Ophthalmol. Vis. Sci.* **55**: 7904–7918.
- Omri, S., B. Omri, M. Savoldelli, *et al.* 2010. The outer limiting membrane (OLM) revisited: clinical implications. *Clin. Ophthalmol.* **4**: 183–195.
- Berkowitz, B.A., R.H. Podolsky, H. Qian, *et al.* 2018. Mitochondrial respiration in outer retina contributes to light-evoked increase in hydration *in vivo*. *Invest. Ophthalmol. Vis. Sci.* **59**: 5957–5964.
- Berkowitz, B.A., R.H. Podolsky, K.M. Lins-Childers, *et al.* 2019. Outer retinal oxidative stress measured *in vivo* using QUEnch-assiSTed (QUEST) OCT. *Invest. Ophthalmol. Vis. Sci.* **60**: 1566–1570.
- Li, J.D., R.P. Gallemore, A. Dmitriev & R.H. Steinberg. 1994. Light-dependent hydration of the space surrounding photoreceptors in chick retina. *Invest. Ophthalmol. Vis. Sci.* **35**: 2700–2711.
- Li, J.D., V.I. Govardovskii & R.H. Steinberg. 1994. Light-dependent hydration of the space surrounding photoreceptors in the cat retina. *Vis. Neurosci.* **11**: 743–752.
- Berkowitz, B.A., E.M. Grady, N. Khetarpal, *et al.* 2015. Oxidative stress and light-evoked responses of the posterior segment in a mouse model of diabetic retinopathy. *Invest. Ophthalmol. Vis. Sci.* **56**: 606–615.
- Zawadzki, R.J., P. Zhang, R.K. Meleppat, *et al.* 2019. Light induced water movement in the outer retina investigated by optical coherence tomography. *Investig. Ophthalmol. Vis. Sci.* **60**: 1294.
- Huang, B. & C.J. Karwoski. 1992. Light-evoked expansion of subretinal space volume in the retina of the frog. *J. Neurosci.* **12**: 4243–4252.
- DeLint, P.J., T.T. Berendschot, J. van de Kraats & D. van Norren. 2000. Slow optical changes in human photoreceptors induced by light. *Invest. Ophthalmol. Vis. Sci.* **41**: 282–289.
- Arshavsky, V. 2002. Like night and day: rods and cones have different pigment regeneration pathways. *Neuron* **36**: 1–3.
- Berkowitz, B.A. 2020. Preventing diabetic retinopathy by mitigating subretinal space oxidative stress *in vivo*. *Vis. Neurosci.* **37**: E002.
- Owsley, C., G. McGwin Jr., M.E. Clark, *et al.* 2016. Delayed rod-mediated dark adaptation is a functional biomarker for incident early age-related macular degeneration. *Ophthalmology* **123**: 344–351.
- Curcio, C.A., N.E. Medeiros & C.L. Millican. 1996. Photoreceptor loss in age-related macular degeneration. *Invest. Ophthalmol. Vis. Sci.* **37**: 1236–1249.

32. Curcio, C.A., C. Owsley & G.R. Jackson. 2000. Spare the rods, save the cones in aging and age-related maculopathy. *Invest. Ophthalmol. Vis. Sci.* **41**: 2015–2018.
33. World Medical Association. 2013. World Medical Association Declaration of Helsinki: ethical principles for medical research involving human subjects. *JAMA* **310**: 2191–2194.
34. Thomas, M.M. & T.D. Lamb. 1999. Light adaptation and dark adaptation of human rod photoreceptors measured from the a-wave of the electroretinogram. *J. Physiol.* **518**: 479–496.
35. Aranha Dos Santos, V., L. Schmetterer, M. Groschl, *et al.* 2015. *In vivo* tear film thickness measurement and tear film dynamics visualization using spectral domain optical coherence tomography. *Opt. Express* **23**: 21043–21063.
36. Dos Santos, V.A., L. Schmetterer, G.J. Triggs, *et al.* 2016. Super-resolved thickness maps of thin film phantoms and *in vivo* visualization of tear film lipid layer using OCT. *Biomed. Opt. Express* **7**: 2650–2670.
37. Zhang, P., B. Shibata, G. Peinado, *et al.* 2020. Measurement of diurnal variation in rod outer segment length *in vivo* in mice with the OCT optoretinogram. *Invest. Ophthalmol. Vis. Sci.* **61**: 9.
38. Srinivasan, V.J., B.K. Monson, M. Wojtkowski, *et al.* 2008. Characterization of outer retinal morphology with high-speed, ultrahigh-resolution optical coherence tomography. *Invest. Ophthalmol. Vis. Sci.* **49**: 1571–1579.
39. Wilk, M.A., B.M. Wilk, C.S. Langlo, *et al.* 2017. Evaluating outer segment length as a surrogate measure of peak foveal cone density. *Vision Res.* **130**: 57–66.
40. Provis, J.M., A.M. Dubis, T. Maddess & J. Carroll. 2013. Adaptation of the central retina for high acuity vision: cones, the fovea and the avascular zone. *Prog. Retin. Eye Res.* **35**: 63–81.
41. Lu, Y.M., B.Q. Wang, D.R. Pepperberg & X.C. Yao. 2017. Stimulus-evoked outer segment changes occur before the hyperpolarization of retinal photoreceptors. *Biomed. Opt. Express* **8**: 38–47.